

Lawrence Berkeley National Laboratory

Recent Work

Title

PION DIFFRACTION DISSOCIATION IN 205 GeV/c n-p INTERACTIONS

Permalink

<https://escholarship.org/uc/item/81q4q0d3>

Authors

Winkelmann, F.C.

Abrams, G.S.

Bingham, H.H.

et al.

Publication Date

1973-10-01

RECEIVED
LAWRENCE
RADIATION LABORATORY

JAN 2 1974

LIBRARY AND
DOCUMENTS SECTION

PION DIFFRACTION DISSOCIATION IN
205 GeV/c π^- p INTERACTIONS

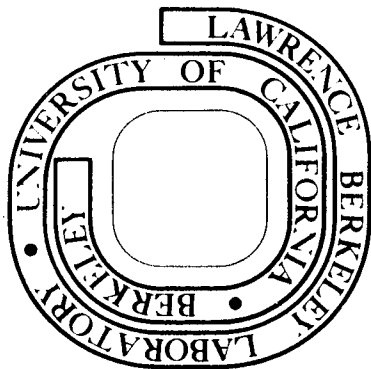
F. C. Winkelmann, G. S. Abrams, H. H. Bingham,
D. M. Chew, B. Y. Daugéras, W. B. Fretter,
C. E. Friedberg, G. Goldhaber, W. R. Graves, A. D. Johnson,
J. A. Kadyk, L. Stutte, G. H. Trilling, G. P. Yost
D. Bogert, R. Hanft, F. R. Huson, D. Ljung,
C. Pascaud, S. Pruss and W. M. Smart

October 1973

Prepared for the U. S. Atomic Energy Commission
under Contract W-7405-ENG-48

For Reference

Not to be taken from this room



DISCLAIMER

This document was prepared as an account of work sponsored by the United States Government. While this document is believed to contain correct information, neither the United States Government nor any agency thereof, nor the Regents of the University of California, nor any of their employees, makes any warranty, express or implied, or assumes any legal responsibility for the accuracy, completeness, or usefulness of any information, apparatus, product, or process disclosed, or represents that its use would not infringe privately owned rights. Reference herein to any specific commercial product, process, or service by its trade name, trademark, manufacturer, or otherwise, does not necessarily constitute or imply its endorsement, recommendation, or favoring by the United States Government or any agency thereof, or the Regents of the University of California. The views and opinions of authors expressed herein do not necessarily state or reflect those of the United States Government or any agency thereof or the Regents of the University of California.

PION DIFFRACTION DISSOCIATION IN 205 GeV/c π^-p INTERACTIONS*

F. C. Winkelmann, G. S. Abrams, H. H. Bingham, D. M. Chew,
 B. Y. Daugéras,[†] W. B. Fretter, C. E. Friedberg, G. Goldhaber,
 W. R. Graves, A. D. Johnson, J. A. Kadyk, L. Stutte,
 G. H. Trilling and G. P. Yost

Department of Physics and Lawrence Berkeley Laboratory
 University of California, Berkeley, California 94720

and

D. Bogert, R. Hanft, F. R. Huson, D. Ljung,
 C. Pascaud,[†] S. Pruss, W. M. Smart

National Accelerator Laboratory, Batavia, Illinois 60510

October 1973

ABSTRACT

Pion diffraction dissociation into masses up to approximately 6 GeV is observed in the reaction $\pi^-p \rightarrow p + X$ at 205 GeV/c. The pion single diffraction cross section for mass-squared $\leq 32 \text{ GeV}^2$ is $1.9 \pm 0.2 \text{ mb}$.

Diffraction dissociation of the pion into states of mass $\lesssim 2 \text{ GeV}$ has been established in pion-nucleon experiments at momenta up to 40 GeV/c. We describe here a study of 205 GeV/c π^-p interactions in which the first evidence is presented for diffraction dissociation of pions into substantially higher masses, up to approximately 6 GeV. Many of the features of pion diffraction dissociation which we will discuss are similar to those recently observed for proton diffraction in pp interactions at NAL and ISR energies.¹

Our results are based on a 48,000-picture exposure of the NAL 30-inch hydrogen bubble chamber. The experimental arrangement, the scanning and measurement of events, and the separation of elastic and inelastic 2-prong events have been described previously.² The data sample to be discussed consists of 1566 inelastic events of the form

$$\pi^-p \rightarrow p + X, \quad (1)$$

where the outgoing proton, identified by ionization, has momentum ≤ 1.4 GeV/c. The mass-squared, M^2 , of X and the momentum transfer, t , to the proton were calculated from measurements of the beam and recoil proton. The observed t -dependence (see below) indicates that biases introduced by the cutoff in proton momentum are negligible up to $M^2 = 180$ GeV². The error in M^2 was determined to be approximately ± 1.3 GeV² from 2-prong events which fit the elastic hypothesis.

Mass distributions and cross sections.—Figures 1(a-e) show the distributions in M^2 for charged multiplicity 2, 4, 6, 8, and ≥ 10 for reaction (1).³ We note that: (1) The inelastic 2-prong events show a large peak centered at $M^2 = 2$ GeV², of full width 4 GeV², with a shoulder extending to about 20 GeV². (2) The 4-prong events show a prominent peak similar in position and width to the 2-prong peak, but extending to about 30 GeV². (3) The 6-prong events show a broad enhancement which rises sharply from threshold and extends to about 30 GeV². (4) The 8-prong events show a less-pronounced enhancement which rises slowly from threshold. (5) For ≥ 10 prongs, no well-defined structure is observed in the mass region below 30 GeV².

We interpret these enhancements as evidence for the presence of diffraction dissociation of the pion into masses up to about 30 GeV² in the 2-, 4-, 6-, and possibly, 8-prong events. To estimate the cross section for pion single diffraction dissociation, we have taken an upper limit of $M^2 = 32$ GeV² for diffraction and have counted events above a smooth hand-drawn background separately for each multiplicity. The background curves used are shown in Fig. 1. Table I gives the cross sections before and after background subtraction. The errors shown take into account statistical uncertainties, as well as uncertainties in background size and shape and in the corrections applied to the data. We obtain an overall pion single diffraction dissociation cross section of 1.9 ± 0.2 mb for $M^2 < 32$ GeV².

At lower energies, pion diffraction has been observed only for $M^2 < 4 \text{ GeV}^2$. Our cross section for this region, $1.0 \pm 0.1 \text{ mb}$, is comparable to corresponding values at lower energies, consistent with the energy independence expected for diffraction. For the high-mass region, $M^2 = 4 \text{ to } 32 \text{ GeV}^2$, we find a pion diffraction cross section of $0.9 \pm 0.2 \text{ mb}$. When pion-nucleon data at higher energy become available, it will be important to determine whether this high-mass part also has an energy dependence consistent with a diffractive interpretation.

Combining Figs. 1(a-e) we obtain $d\sigma/dM^2$ inclusive, shown in Fig. 1(f). The pion diffraction dissociation contribution is given in Fig. 1(g), which is simply $d\sigma/dM^2$ for events with ≤ 8 prongs, after subtraction of non-diffractive background. The curves in Fig. 1(g) show the functional forms $d\sigma/dM^2 \sim M^{-1}$, M^{-2} , and M^{-3} , all normalized to the measured value of $d\sigma/dM^2$ at 10 GeV^2 . A dependence between M^{-2} and M^{-3} reasonably represents the data for $5 \lesssim M^2 \lesssim 40 \text{ GeV}^2$. If the pion diffractive part of reaction (1) is produced by Pomeron exchange, then triple-Regge theory⁴ would predict $d\sigma/dM^2 \sim M^{-2}$ and M^{-3} for PPP and PPR coupling, respectively, where P indicates the Pomeron trajectory and R, the effective meson trajectory.

t-dependence.—The t-dependence of reaction (1) is displayed in Fig. 2 which shows: (a) $d\sigma/dt$ separately for 2-, 4-, 6-, and 8-prongs in the pion diffraction region, $M^2 < 32 \text{ GeV}^2$; and (b) inclusive $d\sigma/dt$ for several ranges of M^2 . All of these distributions have a simple exponential falloff in t. There is no evidence for a turnover in the forward direction (except in $d\sigma/dt$ for $32 < M^2 < 100 \text{ GeV}^2$, where the turnover is consistent with being a kinematic effect associated with minimum allowed momentum transfer). Exponential slopes, b, were obtained by fitting each $d\sigma/dt$ to the form Ae^{bt} . In Fig. 2(a) we find $b \approx 8 \text{ GeV}^{-2}$ with little dependence on charged multiplicity. We see from Fig. 2(b) that b falls rapidly from a value of $9.1 \pm 0.6 \text{ GeV}^{-2}$ for

$M^2 < 4 \text{ GeV}^2$ to about 6.5 GeV^{-2} for M^2 between 4 and 100 GeV^2 . For comparison, the slope for elastic scattering is $9.0 \pm 0.7 \text{ GeV}^{-2}$.

Charged multiplicity.—In Fig. 3(a) we show the charged multiplicity distribution for pion diffraction with $M^2 < 32 \text{ GeV}^2$, and for $\pi^- p \rightarrow$ anything (inelastic). The average charged multiplicity for pion diffraction is 3.8 ± 0.2 , which is about half of the overall average charged multiplicity, 8.02 ± 0.12 .

Figure 3(b) shows the average charged multiplicity, $\langle n_x \rangle$, and dispersion, $D_x = (\langle n_x^2 \rangle - \langle n_x \rangle^2)^{1/2}$, as a function of M^2 for the system X which recoils against the proton in reaction (1). As mentioned before, biases due to the $1.4 \text{ GeV}/c$ cutoff in proton momentum are negligible up to $M^2 = 180 \text{ GeV}^2$. For comparison, Fig. 3(b) also shows the average charged multiplicity, $\langle n_c \rangle$, and dispersion, D_c , for $\pi^- p \rightarrow$ anything (inelastic)⁵ as a function of Q^2 , where, for center-of-mass energy \sqrt{s} , $Q = \sqrt{s} - m_p - m_\pi$. We observe that $\langle n_x \rangle$ and $\langle n_c \rangle$ are remarkably similar over a broad range of energy extending from $M^2 \approx 1$ up to $M^2 \approx 200 \text{ GeV}^2$. The dispersions D_x and D_c are also quite similar, particularly above 10 GeV^2 .

Although our data do not allow a precise determination of the functional dependence of $\langle n_x \rangle$ or D_x on M , we note the following trends: (1) for $M^2 \gtrsim 10 \text{ GeV}^2$, $\langle n_x \rangle$ and D_x are consistent with logarithmic dependences of the form $\langle n_x \rangle = 0.3 + 1.3 \log M^2$ and $D_x = 0.2 + 0.6 \log M^2$ [solid straight lines, Fig. 3(b)]. A $\log M^2$ behavior for $\langle n_x \rangle$ is predicted by triple-Pomeron theory⁶ in the high-mass diffractive region, $10 \lesssim M^2 \lesssim 30 \text{ GeV}^2$, and also by the ABFST multiperipheral model⁷ for $M^2 \gtrsim 20 \text{ GeV}^2$. (2) For the pion-diffractive region as a whole, $\langle n_x \rangle$ is consistent with a power-law dependence of the form $a + bM^n$, with fitted values $a = 1.3 \pm 0.6$, $b = 0.6 \pm 0.4$, and $n = 1.1 \pm 0.4$ for $1 \leq M^2 \leq 32 \text{ GeV}^2$ [dashed curve, Fig. 3(b)]. This is compatible with both the nova model⁸ and the diffractive excitation model,⁹ which predict $n \approx 1$.

It is a pleasure to acknowledge the effort put forth by the 30-inch bubble chamber staff, the hadron beam group, the accelerator operations personnel, and our scanning and measuring staffs. We also wish to thank G. F. Chew, R. Hwa, and H. J. Lubatti for helpful discussions.

FOOTNOTES AND REFERENCES

*Work supported in part by the U. S. Atomic Energy Commission, the National Science Foundation, and French C.N.R.S.

†Permanent address: L.A.L., Orsay, France.

1. For a recent review of high-mass diffractive processes, see D. W. G. S. Leith, Proceedings of the APS Division of Particles and Fields Meeting at Berkeley (1973), and SLAC-PUB-1330 (1973).
2. D. Bogert et al., Phys. Rev. Letters 31, 1271 (1973).
3. Corrections have been applied to the data for scanning and measuring loss of events with short, steeply-dipping protons (10% for 2-prongs, 5% for ≥ 4 -prongs), and for inefficiency in identifying protons with momentum ≤ 1.4 GeV/c (10% for ≤ 8 -prongs, 15% for ≥ 10 prongs). In addition, an M^2 -dependent correction averaging 23% has been applied to the inelastic 2-prong sample with $M^2 < 10 \text{ GeV}^2$ to account for 2-prong inelastic events which fit the elastic hypothesis (see Ref. 2).
4. W. R. Frazer et al., Rev. Mod. Phys. 44, 284 (1972), and references therein.
5. The average charged multiplicity and dispersion for $\pi^- p \rightarrow \text{anything}$ at lower energies were obtained from E. Bracci, CERN/HERA 72-1 (1972), for $P_{\text{LAB}} < 6 \text{ GeV/c}$, and from a compilation by V. V. Ammosov et al., Nucl. Physics B58, 77 (1973), for $P_{\text{LAB}} > 6 \text{ GeV/c}$.
6. W. R. Frazer and D. R. Snider, Phys. Letters 45B, 136 (1973).
7. C.-F. Chan, Phys. Rev. D8, 179 (1973).
8. E. L. Berger, M. Jacob, and R. Slansky, Phys. Rev. D6, 2580 (1972).
9. R. C. Hwa and C. S. Lam, Phys. Rev. D5, 766 (1972).

Table I. Cross sections for $\pi^- p \rightarrow p + X$
with recoil proton momentum ≤ 1.4 GeV/c.

Prongs	$M^2 < 32$ GeV ² , no background subtraction (mb)	Pion single diffraction ^b (mb)	
		$M^2 < 32$	$M^2 < 4$
2 ^a	0.70±0.09	0.67±0.09	0.46±0.07
4	0.97±0.09	0.84±0.08	0.46±0.05
6	0.39±0.05	0.29±0.06	0.04±0.01
8	0.17±0.03	0.10±0.04	0.004±0.004
≥ 10	0.04±0.01	---	---
Totals	2.3±0.2	1.9±0.2	1.0±0.1

^aInelastic only.

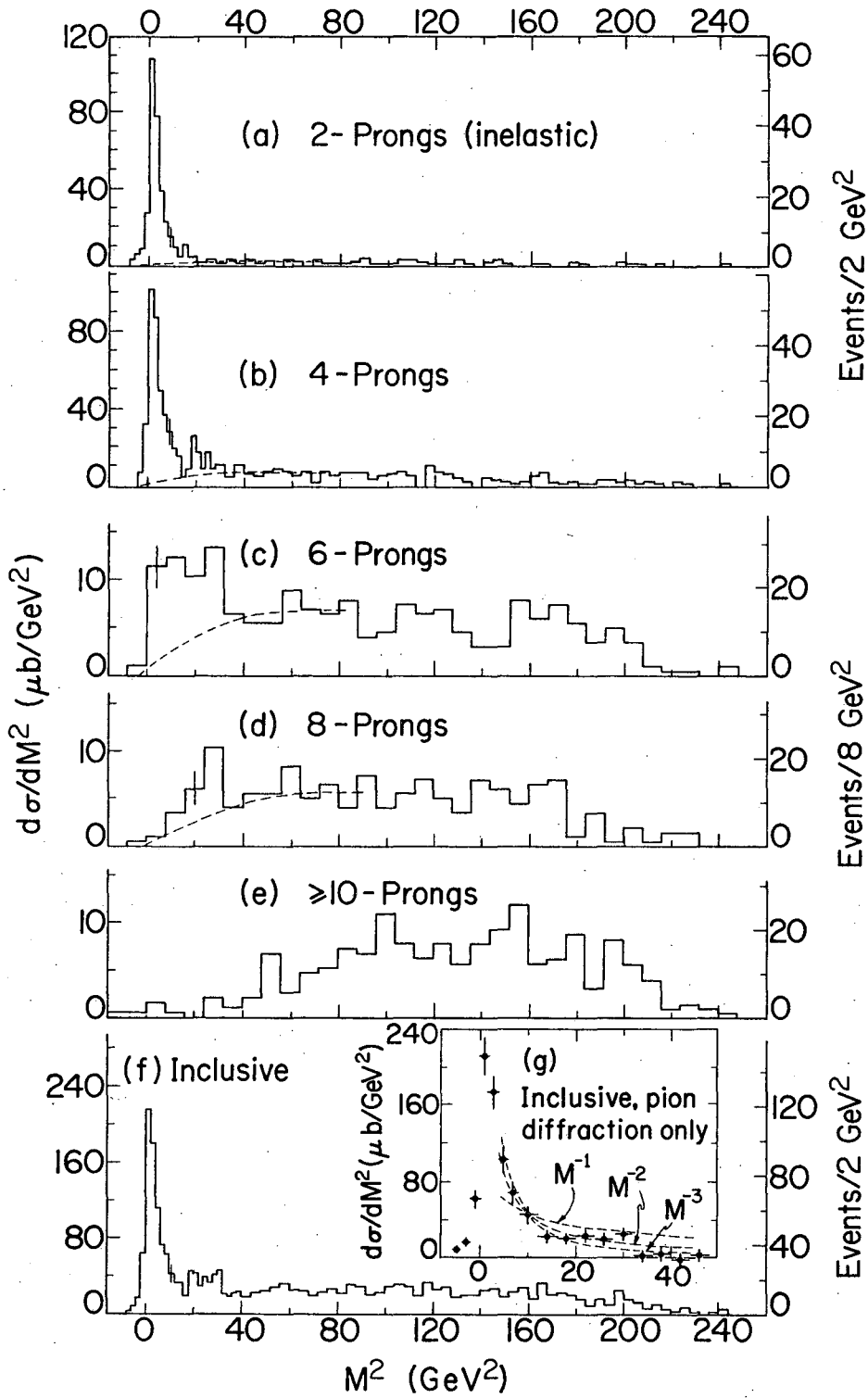
^bAfter background subtraction described in text
(negligible for $M^2 < 4$ GeV²).

FIGURE CAPTIONS

Fig. 1. (a-e) Distributions in M^2 for $\pi^- p \rightarrow p + X$ for inelastic 2-, 4-, 6-, 8- and ≥ 10 -prong events. The dashed curves are estimates of the non-diffractive background. (f) Inclusive M^2 distribution [sum of (a-e)]. (g) Inclusive M^2 distribution for pion diffraction only. The curves show M^{-1} , M^{-2} and M^{-3} dependences normalized to the measured value of $d\sigma/dM^2$ at 10 GeV^2 .

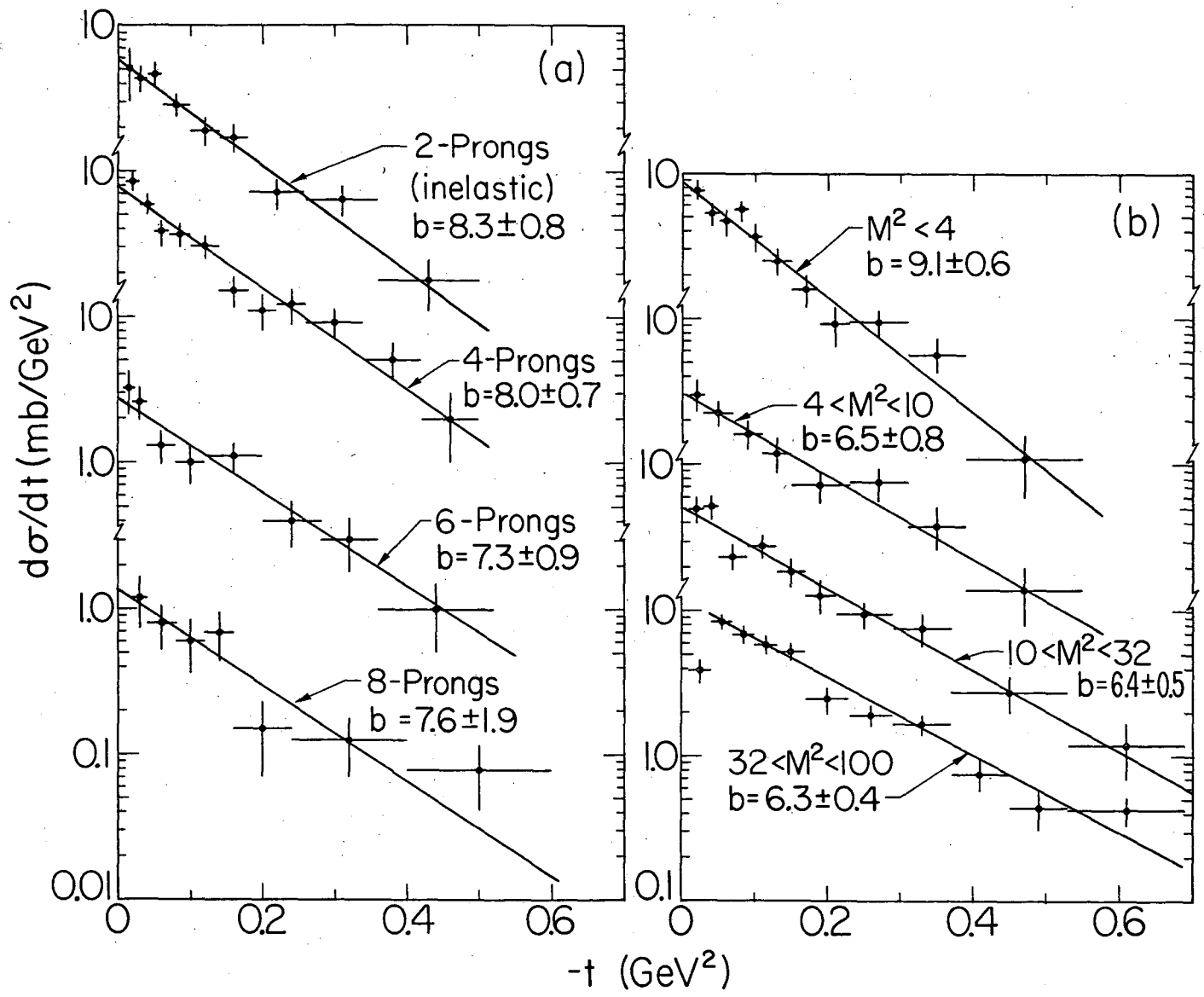
Fig. 2. (a) $d\sigma/dt$ for inelastic 2-, 4-, 6-, and 8-prong events in the pion diffraction region, $M^2 < 32 \text{ GeV}^2$; (b) inclusive $d\sigma/dt$ for several ranges of M^2 . In (a) and (b) the data for $0.01 < -t < 0.03 \text{ GeV}^2$ have been corrected for loss of short, steeply-dipping protons using the observed distribution of the proton azimuthal angle about the beam direction. The straight lines in (a) and (b) show fits to the form Ae^{bt} , yielding the exponential slopes indicated.

Fig. 3. (a) Charged multiplicity distribution at $205 \text{ GeV}/c$ for $\pi^- p \rightarrow$ anything, inelastic (solid curve) and for pion single diffraction dissociation with $M^2 < 32 \text{ GeV}^2$ (dashed curve). The curves have been drawn to guide the eye. (b) Comparison of the energy dependence of the average charged multiplicity and dispersion for the system X in $\pi^- p \rightarrow p + X$, inelastic (\diamond), and for $\pi^- p \rightarrow$ anything, inelastic (\blacktriangle) (Refs. 2 and 5). The horizontal axis for $\pi^- p \rightarrow p + X$ is M^2 and for $\pi^- p \rightarrow$ anything it is Q^2 , the square of the available center-of-mass energy. The dashed curve is a fit to $\langle n_x \rangle$ for $1 \leq M^2 \leq 32 \text{ GeV}^2$ of the form $a + bM^n$, with $n = 1.1 \pm 0.4$, $a = 1.3 \pm 0.6$, and $b = 0.6 \pm 0.4$. The solid straight lines show the functional forms $\langle n_x \rangle = 0.3 + 1.3 \log M^2$ and $[\langle n_x^2 \rangle - \langle n_x \rangle^2]^{1/2} = 0.2 + 0.6 \log M^2$.



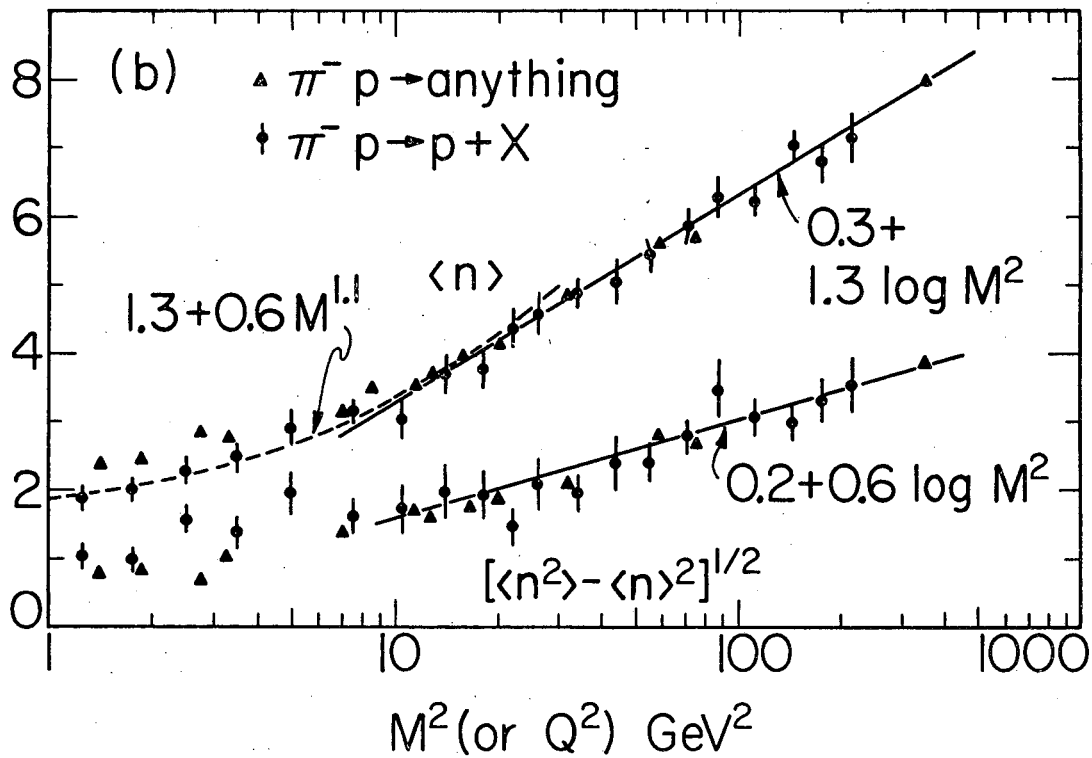
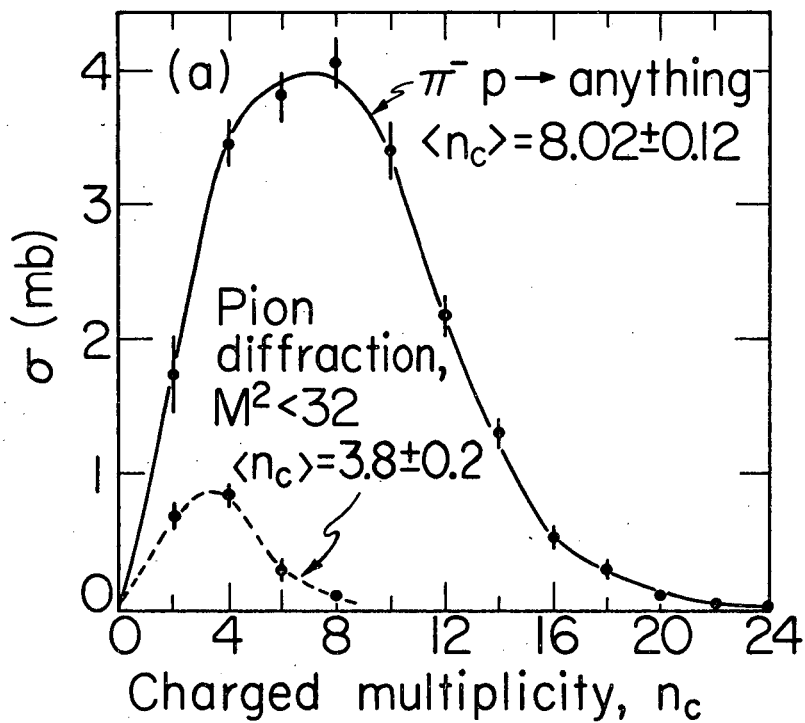
XBL7311-4416

Fig. 1



XBL7311-4415

Fig. 2



XBL7311-4414

Fig. 3

LEGAL NOTICE

This report was prepared as an account of work sponsored by the United States Government. Neither the United States nor the United States Atomic Energy Commission, nor any of their employees, nor any of their contractors, subcontractors, or their employees, makes any warranty, express or implied, or assumes any legal liability or responsibility for the accuracy, completeness or usefulness of any information, apparatus, product or process disclosed, or represents that its use would not infringe privately owned rights.

TECHNICAL INFORMATION DIVISION
LAWRENCE BERKELEY LABORATORY
UNIVERSITY OF CALIFORNIA
BERKELEY, CALIFORNIA 94720